ACS APPLIED MATERIALS & INTERFACES

Research Article

www.acsami.org

Remote Loading of $^{64}Cu^{2+}$ into Liposomes without the Use of Ion Transport Enhancers

Jonas R. Henriksen,[†,⊥] Anncatrine L. Petersen,[‡,⊥] Anders E. Hansen,[‡,§,⊥] Christian G. Frankær,[†] Pernille Harris,[†] Dennis R. Elema,[∥,⊥] Annemarie T. Kristensen,[#] Andreas Kjær,[§] and Thomas L. Andresen*[,‡,⊥]

[†]Department of Chemistry, Technical University of Denmark, Building 206, 2800 Lyngby, Denmark

[‡]Department of Micro- and Nanotechnology, Technical University of Denmark, Building 423, 2800 Lyngby, Denmark

[§]Department of Clinical Physiology, Nuclear Medicine & PET, Faculty of Health Sciences and Cluster for Molecular Imaging, Rigshospitalet, University of Copenhagen, Blegdamsvej 3, 2200 Copenhagen N, Denmark

[∥]DTU Nutech, Hevesy Laboratory, Technical University of Denmark, Frederiksborgvej 399, 4000 Roskilde, Denmark

[⊥]Center for Nanomedicine and Theranostics, Technical University of Denmark, 2800 Lyngby, Denmark

[#]Department of Veterinary Clinical and Animal Sciences, Faculty of Health and Medical Sciences, University of Copenhagen, Dyrlægevej 16, 1870 Frederiksberg C, Denmark

Supporting Information

ABSTRACT: Due to low ion permeability of lipid bilayers, it has been and still is common practice to use transporter molecules such as ionophores or lipophilic chelators to increase transmembrane diffusion rates and loading efficiencies of radionuclides into liposomes. Here, we report a novel and very simple method for loading the positron emitter $^{64}Cu^{2+}$ into liposomes, which is important for *in vivo* positron emission tomography (PET) imaging. By this approach, copper is added to liposomes entrapping a chelator, which causes spontaneous diffusion of copper across the lipid bilayer where it is trapped. Using this method, we achieve highly efficient $^{64}Cu^{2+}$ loading (>95%), high radionuclide retention (>95%), and favorable loading kinetics, excluding the use of transporter molecule additives. Therefore, clinically relevant activities of 200−400 MBq/patient can be loaded fast (60−75 min) and efficiently into preformed stealth liposomes avoiding subsequent purification steps. We investigate the molecular coordination of entrapped copper using X-ray absorption spectroscopy and demonstrate high adaptability of the loading method to pegylated, nonpegylated, gel- or fluid-like, cholesterol rich or cholesterol depleted, cationic, anionic, and zwitterionic lipid compositions. We demonstrate high *in vivo* stability of ^{64}Cu-liposomes in a large canine model observing a blood circulation half-life of 24 h and show a tumor accumulation of 6% ID/g in FaDu xenograft mice using PET imaging. With this work, it is demonstrated that copper ions are capable of crossing a lipid membrane unassisted. This method is highly valuable for characterizing the *in vivo* performance of liposome-based nanomedicine with great potential in diagnostic imaging applications.

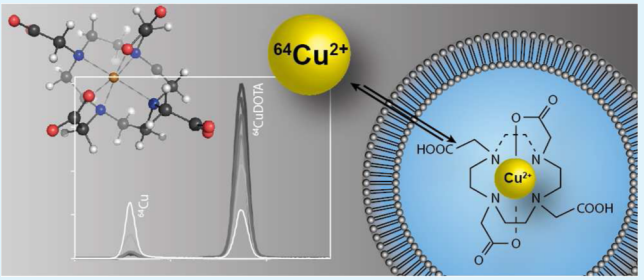

KEYWORDS: *nanoparticles, remote loading, ion permeability, diagnostic, positron emission tomography, molecular imaging*

1. INTRODUCTION

In recent years, the use of imaging in cancer diagnostics and treatment planning has increased considerably. New companion diagnostic agents are emerging[1,2] that can be used to select patients that will be responsive to a specific treatment. Methods for radiolabeling of nanodrugs are particularly interesting as nanomedicines provide new possibilities in companion diagnostics and personalized medicine. A number of radiolabeling methods have already been developed for preparing radioactive liposomes,[3−14] where the main focus has been on single-photon emission computed tomography (SPECT) isotopes. Labeling of liposomes with PET isotopes can provide high-resolution and superior quantitative information on the pharmacokinetics and biodistribution of potential nanodrugs, which can be of high value during drug development and for clinical translation.[1,2] Among the different methods for preparing radioactive liposomes, remote loading of radionuclides into the aqueous core of liposomes seems to provide the greatest *in vivo* stability. The radionuclides reside in a protected environment inside the liposome, which reduce the risk of transmetalation after administration, in comparison to radionuclide surface chelation.[5,6]

Received: May 27, 2015
Accepted: October 1, 2015
Published: October 1, 2015

DOI: 10.1021/acsami.5b04612
ACS Appl. Mater. Interfaces 2015, 7, 22796−22806

Several research groups have investigated the membrane permeability of anions and cations.[15−18] From these studies, low ion permeability of phospholipid bilayers, such as liposomes, is expected to result in highly unfavorable loading kinetics of charged ion species. Common practice is therefore to use ionophores to increase the transmembrane ion diffusion rate and thereby improve the loading kinetics of charged ions such as radionuclides into liposomes.[7−13] Hence, over the last 30 years, ionophores and lipophilic chelators have been used for remote (gradient assisted) loading of radionuclides such as $^{111}In^{3+}$, $^{67/68}Ga^{3+}$, $^{64}Cu^{2+}$, $^{123/124}I^{-}$, $^{177}Lu^{3+}$, and $^{99m}TcO_4^{-}$ into liposomes.[7−12] So far, only a few ionophore assisted loading (IAL) procedures have been developed for liposomal PET imaging applications.[1,12−14] Despite the generally high loading efficiencies, high radionuclide retention, rapid loading kinetics, and successful *in vivo* liposomal performance there are disadvantages of using transporter molecules such as ionophores or lipophilic chelators (hereafter referred to as ionophores as a common term) for remote loading of radionuclides into liposomes. One example is loading of $^{64}Cu^{2+}$ into liposomes using the ionophore, 2-hydroxyquinoline (2HQ), described in our previous work (Figure 1, *right*). In that loading process, the ionophores are stripped from $^{64}Cu^{2+}$ ($Cu(2HQ)_2^{2+} \Leftrightarrow Cu^{2+} + 2\ 2HQ$), which is not a spontaneous process due the high copper affinity of 2HQ.

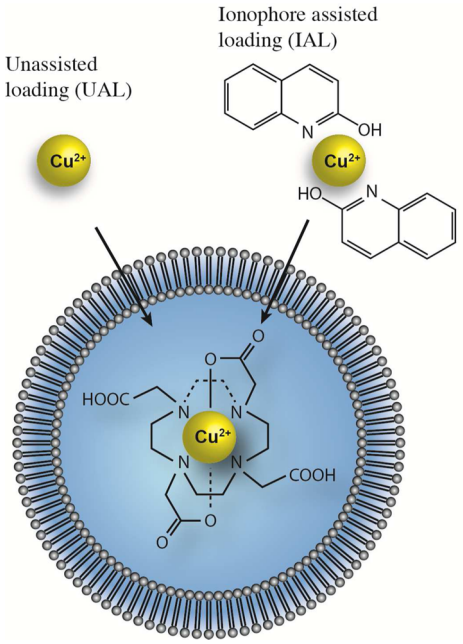

Figure 1. Loading of Cu^{2+} into liposomes. After addition of Cu^{2+} to a liposome solution, Cu^{2+} can pass the lipid bilayer either unassisted (left) or assisted (right) by an ionophore such as 2-hydroxyquinoline (2HQ). Cu^{2+} then forms a complex with the encapsulated chelator (DOTA) and is hereby trapped inside the liposome.

This effect reduces the thermodynamic driving force for forming the radionuclide-chelator complex inside the liposome and thereby potentially the loading efficiency. Thus, choosing a correctly matched entrapped chelator and ionophore with respect to copper affinity is essential for obtaining a thermodynamic stable encapsulation of the radionuclide[12] when using the IAL method. Otherwise, the radionuclide may be prematurely released after *in vivo* administration, which can result in erroneous estimation of the distribution of the liposomes and lowering of PET image quality.

Despite previous knowledge and findings within this field, the present work describes a novel loading method of the PET radionuclide $^{64}Cu^{2+}$ into liposomes, excluding the use of ionophores (an unassisted loading). In this method, $^{64}Cu^{2+}$ (or copper) is added to preformed liposomes entrapping a high affinity copper chelator (Figure 1, *left*). The aqueous core of these liposomes is depleted from free copper due to the presence of the entrapped chelator. This establishes a steep transmembrane copper gradient, which facilitates diffusion of copper ions across the lipid bilayer. Once inside, the encapsulated chelator traps copper. The fact that ionophores can be avoided in the current unassisted loading (UAL) method presents a major advancement with respect to radionuclide entrapment stability and simplicity of loading compared to other and our previous published methods.[12] It is furthermore highly surprising due to the general belief that cation diffusion across lipid bilayers is very slow.

In the present work, the loading efficiency of the new UAL method is compared to our previously published method, which relies on the use of 2-hydroxyquinoline for ionophore assisted transport of Cu^{2+}.[12] In order to characterize and optimize the conditions at which the loading is most favorable, the loading efficiency and loading kinetics, of the UAL method, are investigated as a function of temperature. The UAL method is furthermore tested for several liposome formulations, including ligand-targeted, pegylated, nonpegylated, gel- or fluid-like, cholesterol rich or cholesterol depleted, cationic, anionic, and zwitterionic lipid compositions. The loading of $^{64}Cu^{2+}$ is analyzed using size exclusion chromatography (SEC) and radio thin layer chromatography (radio-TLC).

The UAL method is investigated further by analysis of liposomes loaded with nonradioactive copper. The loading efficiency of these liposomes is analyzed by ICP-MS, and ligands coordinating the liposome-entrapped copper are explored by X-ray absorption spectroscopy.

The *in vivo* performance of ^{64}Cu-loaded liposomes is evaluated in tumor-bearing mice and in a large canine model. Biodistribution and tumor accumulation is quantified using combined PET/computed tomography (CT) imaging.

2. MATERIALS AND METHODS

2.1. Materials. 1,2-Dipalmitoyl-*sn*-glycero-3-phospho-(1′-*rac*-glycerol) (DPPG), 1,2-dipalmitoyl-*sn*-glycero-3-phosphocholine (DPPC), 1-palmitoyl-2-oleoyl-*sn*-glycero-3-phospho-(1′-*rac*-glycerol) (POPG), 1-palmitoyl-2-oleoyl-*sn*-glycero-3-phosphocholine (POPC), 1,2-stearoyl-3-trimethylammonium-propane (DSTAP), hydrogenated soy phosphatidylcholine (HSPC), 1,2-distearoyl-*sn*-glycero-3-phosphocholine (DSPC), cholesterol (CHOL), 1,2-distearoyl-*sn*-glycero-3-phosphoethanolamine-*N*-[methoxy(polyethylene glycol)-2000] (DSPE-PEG_{2000}), and 1,2-distearoyl-*sn*-glycero-3-phosphoethanolamine-*N*-[methoxy(polyethylene glycol)-5000]-Folate (DSPE-PEG_{5000}-Folate) were purchased from Avanti Polar Lipids (Alabama, USA). The freeze-dried lipid mixture (stealth formulation) HSPC:CHOL:DSPE-PEG_{2000} with the molar ratio 56.5:38.2:5.3 was purchased from Lipoid GmbH (Ludwigshafen, Germany). DSPE-PEG_{2000}-RGD was synthesized in our own lab using standard peptide solid phase synthesis. In brief, the linear RGDfPropargyl pentapeptide was synthesized using a 2-chlorotrityl chloride resin and standard Fmoc/HATU methodology. After cleavage from the resin, the peptide was cyclized using diphenyl phosphoryl azide and purified by semipreparative HPLC employing a Waters Xterra C18 5 μm (19 × 150 mm) column. Conjugation of the peptide to the PEG-lipid was achieved by standard click-chemistry using copper(II) sulfate. The final product was purified using

DOI: 10.1021/acsami.5b04612
ACS Appl. Mater. Interfaces 2015, 7, 22796−22806

semipreparative HPLC employing a Waters Xterra C8 5 μm (19 × 150 mm) column and was >98% pure based on analytical HPLC and Maldi-TOF MS analysis. 1,4,7,10-Tetraazacyclododecane-1,4,7,10-tetraacetic acid (DOTA) was purchased from Macrocyclics (Dallas, USA). The buffer 4-(2-hydroxyethyl)piperazine-1-ethanesulfonic acid (HEPES) and all other solvents and chemicals were purchased from Sigma-Aldrich (Schnelldorf, Germany) and were used without further purification. Amicon Ultra-15 centrifugal filter units were purchased from Millipore (Denmark). TLC-plates Silica gel 60 F_{254} were purchased from Merck (Darmstadt, Germany). Mini-extruder was purchased from Avanti Polar Lipids (Alabama, USA). LIPEX Thermobarrel Pressure Extruder (10 mL) was purchased from Northern Lipids (Burnaby, Canada), and the Minimate tangential flow filtration system was purchased from Pall Corporation (Canada). Human serum was purchased from Sigma-Aldrich (Schnelldorf, Germany). Mice and dog blood was taped from animals into Hirudine tubes, and the plasma fraction was collected.

2.2. ^{64}Cu Production. Copper-64 was produced on a PETtrace cyclotron (GE Healthcare). The production of $^{64}Cu^{2+}$ was carried out via the $^{64}Ni(p,n)^{64}Cu$ nuclear reaction as described previously.[12] A specific activity of 3.3 TBq/μmol (Cu) was achieved on average corresponding to 36% radioactive Cu nuclides (^{64}Cu/Cu). The $^{64}CuCl_2$ was isolated by evaporation of aqueous 1 M HCl to dryness once added to a vial and used hereafter for remote loading of liposomes.

2.3. Preparation of Liposomes. *Chelator-Containing Liposomes Were Prepared as Follows.* The lipids were mixed in a chloroform:methanol (9:1) mixture and dried to a lipid-film under a gentle stream of nitrogen. Organic solvent residues were removed under reduced pressure overnight. As an exception, the HSPC:CHOL:DSPE-PEG_{2000} (56.5:38.2:5.3) lipid formulation (stealth formulation) was prepared directly from the freeze-dried powder. The lipid-film or the powder was dispersed by adding a hydration buffer (10 mM HEPES, 150 mM NaCl) containing the chelator, DOTA (10 mM). Hydration buffers were adjusted to either pH 4.0 or 7.4 using NaOH and/or HCl resulting in an osmolarity of 330−380 mOsm/kg. Lipid suspensions were prepared at 50−65 mM and hydrated at 65 °C for 60 min. Multilamellar vesicles (MLVs) were sized to large unilamellar vesicles (LUVs) by multiple extrusions through 100 nm polycarbonate filters using an Avanti mini-extruder or a LIPEX Thermobarrel Pressure Extruder (at 10−15 bar nitrogen).

Unencapsulated DOTA was removed by repeated buffer exchange using Amicon Ultra-15 centrifugal filter units (100 kDa cutoff) exchanging the external buffer with a HEPES buffer (10 mM, 150 mM NaCl, pH 7.4, 295 mOsm/kg). In brief, 0.5 mL liposomes (50 mM) were diluted to a total volume of 12 mL using HEPES buffer, and 11 mL were spun through the filter. The spin filtration was repeated four times, and the purified liposomes were collected. It is important to note that repeated filtration is crucial for achieving high loading efficiency (>95%) and fast loading kinetics, since the presence of chelating components on the liposome exterior lowers the copper transmembrane gradient, which slows down the loading kinetics and reduces the overall loading efficiency. The HSPC:CHOL:DSPE-PEG_{2000} (56.5:38.2:5.3) liposome formulation was as an exception purified using a Minimate tangential flow filtration system. After purification, a 100 nm diameter stealth liposome formulation (10 mM lipid entrapping 10 mM DOTA) contains ∼200 μM DOTA (theoretical estimate based on an average lipid cross sectional area of 40 Å^2, and spherical liposome geometry). Since 1 GBq/mL $^{64}Cu^{2+}$ ∼ 1 μM Cu (assuming 10% specific activity), such liposomes are able to load $^{64}Cu^{2+}$ at 2 GBq/mL while still having a 100-fold excess of DOTA.

Empty Liposomes Were Prepared as Follows. The lipid-film or powder was dispersed in aqueous buffer (10 mM HEPES, 150 mM NaCl, pH 7.4, 295 mOsm/kg). The lipid suspension was hydrated at 65 °C for 60 min. MLVs were sized to LUVs by multiple extrusions through 100 nm polycarbonate filters using an Avanti mini-extruder or a LIPEX Thermobarrel Pressure Extruder (at 10−15 bar nitrogen).

All liposome preparations were analyzed for size and zeta-potential using a Zeta Potential analyzer (ZetaPALS, Brookhaven, SE) and phosphor concentration using ICP-MS (Thermo Scientific, iCAP Q).

2.5. Unassisted Loading (UAL) of ^{64}Cu into Liposomes. Purified chelator-containing liposomes (0.5−5.0 mL, 5−50 mM, internal pH 7.4) were added to a capped vial containing radioactive $^{64}CuCl_2$ (50−1500 MBq) in either dry or solvated form (in HEPES buffer). The sample was constantly stirred in a thermostated lead-container during incubation. Unassisted loading (UAL) was conducted by sample incubation for 60−75 min at 25−55 °C. Formulations used for *in vivo* experiments were loaded at 55 °C for 75 min. No change in liposome size or PDI was observed upon loading of the liposomes.

2.6. Ionophore Assisted Loading (IAL) of $^{64}Cu^{2+}$ into Liposomes. In experiments using the ionophore 2-hydroxyquinoline (2HQ) for ionophore assisted loading (IAL) of $^{64}Cu^{2+}$ into chelator-containing liposomes, 10 μL of 2HQ in Milli-Q water (C_{2HQ} = 0.314 mM) were added to the vial containing radioactive $^{64}Cu^{2+}$ prior to addition of chelator-containing liposomes as previously reported.[12] Subsequently, purified chelator-containing liposomes (internal pH 4.0) were added, and loading proceeded as described for the UAL method. No change in liposome size or PDI was observed upon loading of the liposomes.

2.7. $^{64}Cu^{2+}$ Loading Efficiency Measured by Size Exclusion Chromatography (SEC). $^{64}Cu^{2+}$ loading efficiency was measured using size exclusion chromatography (SEC). The fraction of unentrapped ^{64}Cu-DOTA, in the ^{64}Cu-liposome solution, was quantified by separating ^{64}Cu-DOTA from ^{64}Cu-liposomes using a Sephadex G-25 column (1 × 25 cm) eluted with a HEPES buffer (10 mM, 150 mM NaCl, pH 7.4) with an injection volume of 500 μL and a flow rate of 4 mL/min. The ^{64}Cu-liposomal fraction was collected between 20 and 70 min and the ^{64}Cu-DOTA or $^{64}Cu(2HQ)_2$ fraction between 70 and 100 min. An inline radioactivity detector was used for monitoring the SEC elution profile. The radioactivity in the liposomal fraction (A_{lip}) as well as the total sample activity ($A_{tot,SEC}$) was measured in a dose calibrator (Veenstra VDC-505). The loading efficiency was calculated as the ratio of the decay-corrected liposomal fraction and total sample activity, $\%load_{SEC} = 2A_{lip}\exp(\Delta t/T_{1/2})/A_{tot,SEC}$, where $\Delta t \sim 70-80$ min is the time difference between the measurement of A_{lip} and A_{tot}, and $T_{1/2}$ = 12.7 h is the half-life of ^{64}Cu.

The loading efficiency of DSPC:CHOL:DSPE-PEG_{2000} (55:40:10) liposomes entrapping DOTA was investigated using SEC. The loading experiment was conducted at 30, 40, and 50 °C using the new UAL method and our previously reported IAL method.[12] Empty liposomes composed of DSPC:CHOL:DSPE-PEG_{2000} (55:40:10) were included as control in this study.

2.8. $^{64}Cu^{2+}$ Loading Efficiency and Kinetics Measured by Thin Layer Chromatography (Radio-TLC). Free $^{64}Cu^{2+}$ binds to the Sephadex column and hence cannot be quantified by SEC. The fraction of free $^{64}Cu^{2+}$ in the ^{64}Cu-liposome solution was therefore quantified by separation of ^{64}Cu-DOTA and $^{64}Cu^{2+}$ by radio-TLC. Briefly, a 2 μL sample was spotted on a TLC plate (Silica gel 60 F_{254}), and 10% aqueous ammonium acetate:methanol (50:50) was used as eluent. The retention factor (R_f) of ^{64}Cu-DOTA was 0.3−0.4, while $^{64}Cu^{2+}$ remains at the origin (R_f = 0). The TLC plate was read by a radio-TLC scanner (MiniGita Star GM, Raytest) or a Phosphor-imager (Cyclone Plus, PerkinElmer). The radioactive peaks were integrated using associated computer software. The loading efficiency was calculated as $\%load_{TLC} = A_{Cu-DOTA}/A_{tot,TLC}$, where $A_{Cu-DOTA}$ is the ^{64}Cu-DOTA TLC peak activity and $A_{tot,TLC}$ is the total $^{64}Cu^{2+}$ radioactivity deposited on the TLC plate. Since the ^{64}Cu-liposomes collapse once dried on the TLC silica gel, the ^{64}Cu-DOTA TLC-peak corresponds to the total radioactivity associated with DOTA in the sample (including encapsulated and unencapsulated ^{64}Cu-DOTA if present). As a control of the TLC assay, 1 μL of free $^{64}Cu^{2+}$ and 1 μL of DOTA-containing liposomes (without $^{64}Cu^{2+}$) were spotted on top of each other on a TLC plate, and the TLC plate was developed. Since no detectable ^{64}Cu-DOTA was present on the TLC plate in this control, it was ruled out that DOTA reacts with $^{64}Cu^{2+}$ on the TLC plate. The possibility of an erroneous estimation from further complexation of free $^{64}Cu^{2+}$ and DOTA on the TLC plate was

DOI: 10.1021/acsami.5b04612
ACS Appl. Mater. Interfaces 2015, 7, 22796−22806

therefore eliminated, and the method was concluded valid for measuring free $^{64}Cu^{2+}$ in ^{64}Cu-liposome solutions.

The loading kinetics of HSPC:CHOL:DSPE-PEG$_{2000}$ (56.5:38.2:5.3) liposomes were investigated using TLC at 25, 40, and 55 °C. First, $^{64}CuCl_2$ was dissolved in buffer (10 mM HEPES, 150 mM NaCl, pH 7.4) at 200 MBq/mL. Second, 100 μL of 9.4 mM liposomes were equilibrated at the target temperature (25, 40, or 55 °C) in an acid washed HPLC vial with constant stirring. The experiments were initiated by adding 100 μL of $^{64}Cu^{2+}$ solution (equilibrated at the target temperature), and TLC spots were deposited after 1, 3, 8, 15, 30, and 60 min. The TLC plate was subsequently developed as described above. No challenging reagents such as EDTA were required for quantification of the active loading as the current HPLC and TLC assays are able to quantify the amount of free ^{64}Cu-DOTA and free ^{64}Cu with satisfactory accuracy and precision.

2.9. X-ray Absorption Spectroscopy of Nonradioactive Cu-Loaded Liposomes. Liposomes were prepared from HSPC:CHOL:DSPE-PEG$_{2000}$ (56.5:38.2:5.3), by hydration of lipid powder in a solution of 10 mM HEPES and 100 mM DOTA (pH 7.4, 325 mOsm/kg). These liposomes were prepared with a higher copper loading capacity entrapping 100 mM DOTA (internal liposome concentration) and were extruded and purified as described in section 2.3.

The liposomes were loaded with nonradioative copper (Cu) by mixing with $CuCl_2$ dissolved in aqueous buffer (10 HEPES mM, 150 mM NaCl, pH 7.4). First, 400 μL of liposomes (entrapping 100 mM DOTA) was mixed with 66 μL of a $CuCl_2$ solution (6.2 mM). Second, the liposome−copper mixture was incubated in a closed vial at 55 °C for 2 h, and the sample was shaken gently regularly. Finally, the sample was equilibrated at room temperature.

The loading efficiency was measured by ICP-MS (Thermo Scientific, iCAP Q). This was accomplished by mixing 10 μL of a Cu-loaded liposome sample with 40 μL of EDTA (1 mM) (dissolved in HEPES buffer, pH adjusted to 7.4) and 950 μL of HEPES buffer. The sample was incubated at room temperature for 15 min, and the total Cu content of the EDTA spiked sample was determined by a 100-fold dilution of the sample in 3% HNO_3 solution (spiked with 25 ppb Ga as internal standard). The Cu content of the liposome exterior was determined via spin filtration of the EDTA spiked sample. Briefly, 950 μL of EDTA spiked sample was transferred to an Amicon Ultra-15 centrifugal filter unit (100 kDa cutoff), which was spun at 1000 g for 15 min, or until 250 μL had passed the filter. Following, filtrate was diluted 100-fold with 3% HNO_3 solution (spiked with 25 ppb Ga as internal standard). The copper content of the unfiltered sample and sample filtrate were quantified by ICP-MS, and the loading efficiency was calculated as the ratio of filtrate and total copper content. The recovery of copper for the spin filtration method was tested by conducting loading experiments with either no or empty liposomes not entrapping any chelator using matching conditions as for loading of the DOTA-liposomes.

Copper K-edge X-ray absorption spectra were recorded for solvated Cu (790 μM $CuCl_2$ in 10 mM HEPES, 150 mM NaCl, pH 7.4), Cu-DOTA (790 μM $CuCl_2$, 1.0 mM DOTA in 10 mM HEPES, 150 mM NaCl, pH 7.4), and Cu-loaded liposomes (720 μM $CuCl_2$) on beamline I811 at the MAX-II synchrotron at MAXIV Laboratory, Lund, Sweden,[19] using a Si(111) double-crystal monochromator. The samples were mounted in 1 mm thick sample holders[20] and cooled to 20 K in a liquid helium cryostat. Fluorescence data were collected using a Vortex silicon-drift detector (50 mm^2) in the XANES region 8830−9180 eV. Five to ten scans of 25 min were recorded for each sample in the following intervals: pre-edge data (150−20 eV before the edge) were collected in steps of 5 eV for 1 s, the edge (from 20 eV before to 30 eV above the edge) in steps of 0.3 eV for 1 s, the XANES region (30−120 eV above the edge) in steps of 1 eV for 1 s, and the NEXAFS region (120−200 eV above the edge) in steps of 5 eV for 3 s. Comparing successive scans, no photo reduction or radiation damage of the samples were observed.

The scans were, averaged, background subtracted, normalized, and energy calibrated using WinXAS.[21] Full multiple scattering calculations of XANES spectra by finite-difference methods (FDM) were performed using FDMNES[22] on clusters with a radius of 4.5 Å of the Cu-atom. The fit between calculated and experimental spectra was evaluated with an R factor given as

$$R_{\mathrm{XANES}} = \frac{\sum |\mu^{\mathrm{exp}}(E) - \mu^{\mathrm{cal}}(E)|}{\sum |\mu^{\mathrm{exp}}(E)|} \quad (1)$$

where μ is the absorption/fluorescence yield from normalized XANES spectra as a function of energy, E.

2.10. Animal Xenograft Model. Human FaDu head and neck cancer cells (5 × 10^6 cells in 100 μL of media and matrigel) were inoculated subcutaneously in the flanks of female NMRI nude (Taconic, Borup, Denmark) mice (n = 5) and were allowed to grow 14 days (tumor sizes <0.5 g). All animal experiments were approved by the Danish Animal Welfare Council, Ministry of Justice. ^{64}Cu-liposome suspensions were intravenously injected (*i.v.*) for PET imaging. All animals were anesthetized with sevofluran, and each animal was injected in the tail vein with 200 μL of liposome formulation (3.3 mM lipid, 60 MBq/mL) corresponding to 20 mg lipid/kg and an activity dose level of 12 MBq/animal. PET data were acquired on a MicroPET Focus 120 (Siemens Medical Solutions, Malvern, PA, USA). The voxel size was 0.866 × 0.866 × 0.796 mm^3, and in the center field of view the resolution was 1.4 mm full width at half-maximum (fwhm). PET scans were acquired 5 min after injection of radiolabeled liposomes (scan time 5 min) and again 24 h after injection (scan time 15 min). Data were reconstructed with the maximum a posterior (MAP) reconstruction algorithm. For anatomical localization of activity, CT images were acquired with a MicroCAT II system (Siemens Medical solutions, Malvern, PA, USA).

After data reconstruction, PET and CT images were fused using the Inveon Software (Siemens). The emission scans were corrected for random counts and dead time. The PET and CT images were used to identify regions of tracer uptake and to generate regions of interest (ROIs) that were applied to each scan separately. The blood activity was estimated from a spherical ROI constructed within the left heart ventricle. This ROI was subsequently segmented into a blood activity ROI consisting only of voxels displaying minimum 80% of maximum voxel activity of the original ROI. Liposomal activity within each organ was determined from ROIs placed within the border of the investigated organs. ROIs were placed to ensure sufficient organ coverage without compromising the influence of partial volume effects or respiratory movements. The liposomal accumulation in the different organs was expressed as percentage of injected dose per gram (%ID/g) as well as standardized uptake value (SUV).[23] The organ density was assumed to be 1 g/cm^3 for all tissues and tumors. As the utilized stealth liposomes are not actively targeted to any specific cell line, and accumulate passively in tumors based on the EPR effect, no specific cell uptake/internalization evaluation was performed.

2.11. Biodistribution and Circulation Properties in a Clinical Canine Model. A large breed dog (Great Dane, male, 48 kg) underwent ^{64}Cu-liposome PET/CT scanning following a previous surgical removal of a neuroblastoma to evaluate the presence of metastatic or residual cancerous tissue. The study was approved by the Ethical Committee at Dept. Small Animal Clinical Sciences at University of Copenhagen in Denmark. The dog was injected with 2 mg/kg of dexamethasone disodium phosphate approximately 2 h prior to infusion of ^{64}Cu-liposomes to minimize risks of immunologic reactions. ^{64}Cu-liposomes were infused over a 20 min period at increasing infusion rates, and a total of 402.7 MBq of ^{64}Cu-liposomes was infused, equaling a mean lipid concentration of 4.3 mg/kg. EDTA stabilized blood samples were collected at multiple time points during a 24-h period. Blood samples were weighed and well-counted in triplicates, and specific decay corrected injected activity was determined from an expected blood volume (8% of bodyweight).

After a distribution period of 24 h the dog was anesthetized, and a whole body PET/CT scan performed to evaluate biodistribution of the ^{64}Cu-liposomes and the presence of detectable metastatic or residual disease. PET/CT scans were performed using a combined clinical PET/CT scanner dedicated for PET scanning of humans (Biograph 40

DOI: 10.1021/acsami.5b04612
ACS Appl. Mater. Interfaces 2015, 7, 22796−22806

PET/CT) consisting of a high resolution PET scanner (21.6 cm axial field) and a 40-row multislice CT scanner. Images were reconstructed using a 3D acquisition mode and attenuation corrected using the concurrent CT scan. PET images were acquired using 2.5 min per bed positions and reconstructed using TrueX (Siemens, Erlangen, Germany) 3D reconstruction (21 iterations, 3 subsets) and smoothed using a Gaussian filter having a fwhm of 2 mm in all directions and a matrix size of 336 × 336. Dynamic scanning of the canine model was not performed, as the axial PET field of view of the scanner is limited to 20 cm, which prohibits simultaneous scans of several regions of interest. Furthermore, since the dog was privately owned, scans were only acquired to carry diagnostic information, and it was considered unethical to perform a dynamic scan over a period of several hours.

Image analysis of attenuation corrected and reconstructed PET/CT images were performed using commercial software (Pmod, Pmod Technologies, Switzerland). The acquired images revealed no signs of residual or metastatic cancerous tissue. ^{64}Cu-liposome activity in the blood, liver, spleen, and muscle 24 h after ^{64}Cu-liposome infusion were evaluated by constructing reference ROIs using the methodology described above and reported as %ID/g. All regions were drawn well within the margins of tissues and organs and, excluding regions containing larger blood vessels, *e.g.* the hilar region of the liver, to avoid artifacts and minimize partial volume effects and respiratory movement.

2.12. *In Vitro* Stability of ^{64}Cu-Liposomes in Serum. *In vitro* stability of ^{64}Cu-liposomes, prepared by the UAL method, was tested in human serum and canine and mice plasma. Liposomes loaded with 500 MBq ^{64}Cu/mL were mixed with serum or plasma in a 1:1 ratio and incubated for 18 h at 37 °C. The liposome-serum/plasma mixture (200 μL) was separated on a size-exclusion column (Sephadex G50 fine, 25 × 1.5 cm, flow rate 1 mL/min), and fractions were collected every second min. The ^{64}Cu activity of the different fractions was measured using a calibrated high-purity germanium detector (Princeton, Gammatech). Each sample was placed in a distance of 20 cm measured from the surface of the detector crystal. Energy and efficiency calibrations were performed prior to measuring using certified sealed radioactive sources of ^{133}Ba and ^{152}Eu. The spectra were obtained and analyzed using Canberra Genie2K software. The ^{64}Cu activity of each sample was determined by integration of the 511 keV annihilation peak, and the activities were calculated based on the 20 cm efficiency calibration. ^{64}Cu-DOTA was included as a control to determine retention-time (fraction range) of the liposome encapsulated and free ^{64}Cu-DOTA. The leakage of ^{64}Cu-DOTA from the liposomes in serum or plasma was calculated as leakage = $\Sigma_{i=13}^{25} A_{\text{frac}}^{i} / \Sigma_{i=1}^{25} A_{\text{frac}}^{i}$, where A_{frac}^{i} is the activity of the ith fraction (see Supporting Information Figure S1).

3. RESULTS

3.1. Loading of ^{64}Cu^{2+} Evaluated by SEC. In the present work, loading of ^{64}Cu^{2+} into DSPC:CHOL:DSPE-PEG$_{2000}$ (50:40:10) liposomes was tested using an UAL and an IAL method, which are schematically illustrated in Figure 1. The two loading methods are compared by the overall loading efficiency (%load$_{\text{sec}}$) determined using SEC (Figure 2A), which for IAL using 2HQ (Figure 2B) shows an increase from 83% to 92% (11% relative increase) in response to raising the temperature from 30 to 50 °C. In contrast, the UAL method (without 2HQ) shows an increase from 47% to 97% (>100% relative increase) in response to raising the temperature from 30 to 50 °C (Figure 2B).

The largest difference in loading efficiency, between the two loading methods, is observed at 30 and 40 °C. Furthermore, 2HQ is observed to reduce the maximal achieved loading from 97% ± 1% to 92% ± 1%. As control, loading of empty liposomes (without DOTA encapsulated) was carried out using the method described above and showed loading efficiencies of 1% ± 1% and 5% ± 1% for 5 mM and 50 mM

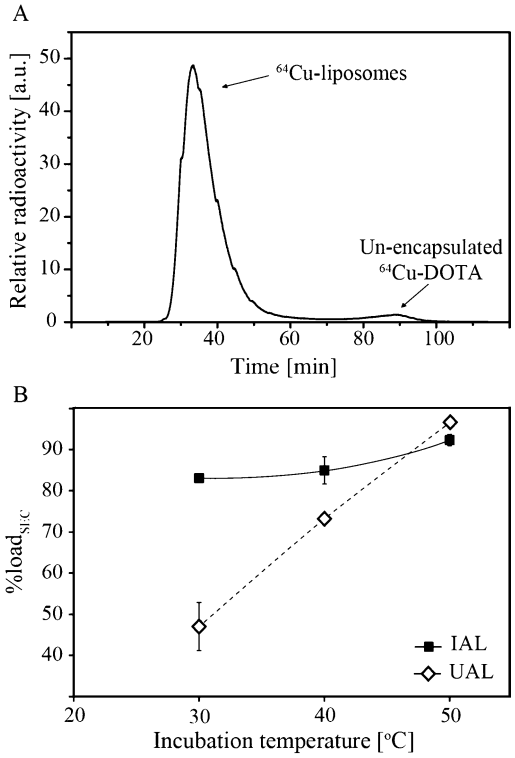

Figure 2. Evaluation of ^{64}Cu^{2+} loading into DOTA-liposomes using size exclusion chromatography (SEC). (A) A typical SEC elution profile of ^{64}Cu^{2+} remote loaded liposomes. (B) Loading efficiency presented as a function of temperature for the unassisted (UAL) and ionophore assisted (IAL) remote loading. The liposomes were incubated for 60 min before SEC analysis. The liposomes were composed of DSPC:CHOL:DSPE-PEG$_{2000}$ in the molar ratio (50:40:10) with the chelator (DOTA) entrapped. The solid and dashed lines serve to guide the eye. The error bars show the standard error of the mean (n = 3) and are not shown for error bars smaller than the symbols.

DSPC:CHOL:DSPE-PEG$_{2000}$ (50:40:10) lipid formulations, respectively, when incubated for 1 h at 55 °C.

3.2. Loading Kinetics of ^{64}Cu^{2+} Evaluated by Radio-TLC. The kinetics of loading ^{64}Cu^{2+} into liposomes, utilizing the new UAL method, was evaluated using radio-TLC (Figure 3A). Loading experiments were conducted at 25, 40, and 55 °C, using HSPC:CHOL:DSPE-PEG$_{2000}$ (56.5:38.2:5.3) liposomes (Figure 3B).

Slow loading kinetics is observed at room temperature (25 °C), where a maximal loading efficiency of 36% ± 4% is reached after 60 min. At 40 °C, loading kinetics is faster, and a maximal loading efficiency of 88% ± 1% is reached after 60 min. The fastest loading is observed at 55 °C, where 97% ± 1% loading is reached after 60 min. The initial velocity of the ^{64}Cu^{2+} loading reaction, judged by the degree of loading achieved after 1 min, increases from 5% ± 1% at 25 °C to 12% ± 1% at 40 °C and reaches 38% ± 3% at 55 °C. A temperature increase of 30 °C thus results in a 8-fold increase in initial loading rate.

3.3. Remote Loading of Nonradioactive Cu and X-ray Absorption Spectroscopy Analysis. The coordination chemistry of copper was investigated using X-ray absorption spectroscopy (XAS) in order to elucidate copper species present in HEPES buffer, HEPES buffer containing DOTA, and in remote loaded liposomes prepared using the UAL method.

DOI: 10.1021/acsami.5b04612
ACS Appl. Mater. Interfaces 2015, 7, 22796−22806

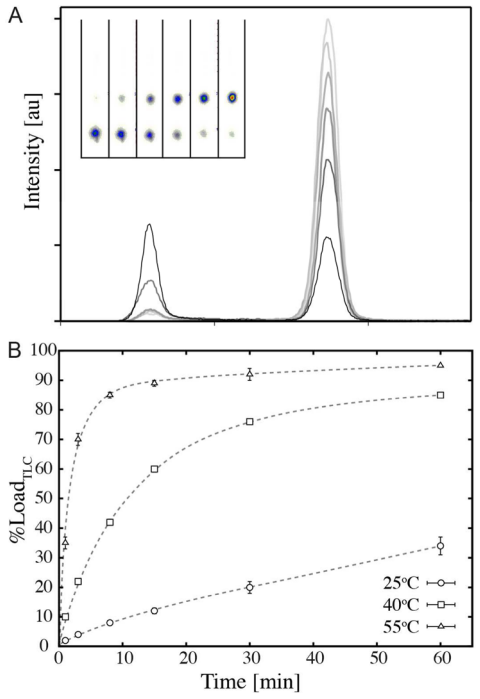

Figure 3. Loading efficiency of liposomes given as a function of time for the UAL method. The loading efficiency, for loading of $^{64}Cu^{2+}$ into liposomes, is evaluated at 25, 40, and 55 °C by the use of radio-TLC. (A) TLC elution profile as a function of time (1, 3, 8, 15, 30, and 60 min) showing the unloaded ($^{64}Cu^{2+}$) and loaded (^{64}Cu-DOTA) copper fractions. The corresponding TLC plate is shown as an inset in panel A. (B) Degree of loading $^{64}Cu^{2+}$ into liposomes (%load$_{TLC}$). The liposomes were composed of HSPC:CHOL:DSPE-PEG$_{2000}$ in the molar ratio (56.5:38.2:5.3). The dashed lines in B serve to guide the eye. The error bars show the standard error of the mean (n = 3) and are not shown for error bars smaller than the symbols.

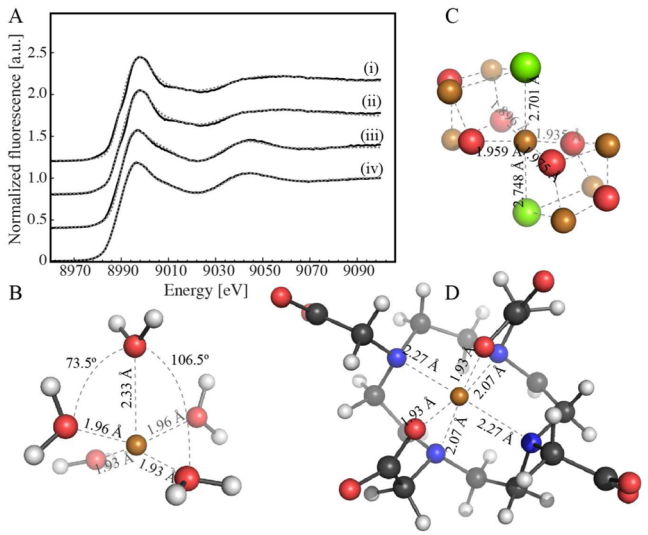

Figure 4. Experimental (solid line) and calculated (dashed) XANES spectra (panel A). From top: (*i*) Solvated Cu^{2+} fitted with a five-coordinate water complex, (*ii*) solvated Cu^{2+} fitted with clinoatacamite, (*iii*) Cu-DOTA fitted with Cu-DOTA complex, and (*iv*) copper loaded liposome fitted with a linear combination of experimental spectra of Cu-DOTA and solvated Cu^{2+}. (B–D) The atomic models used in the calculations of XANES spectra including distances to atoms in the first coordination shell. Panel B shows $[Cu(H_2O)_5]^{2+}$ used to model the solvated Cu^{2+} in HEPES. (C) The most abundant Cu coordination in clinoatacamite, which was also used to model the solvated Cu^{2+} in HEPES. The $[Cu(OH)_4Cl]^{4-}$ complex is shown with the nearest neighbor copper atoms. (D) Cu-DOTA complex. Color code: copper (brown), chlorine (green), oxygen (red), nitrogen (blue), carbon (black), and hydrogen (white).

Therefore, HSPC:CHOL:DSPE-PEG$_{2000}$ (56.5:38.2:5.3) liposomes, entrapping 100 mM DOTA, were mixed with nonradioactive copper (Cu). Sample incubation was conducted at 55 °C for an extended period of time (2 h) to facilitate loading of the larger amount of copper, compared to loading of $^{64}Cu^{2+}$. The liposome sample was examined using ICP-MS, which resulted in a total copper content of 720 μM and an encapsulation efficiency of 93%. Loading of HSPC:CHOL:DSPE-PEG$_{2000}$ (56.5:38.2:5.3) liposomes, entrapping no chelator, resulted in 5% loading. The recovery of copper from the spin filters has furthermore been analyzed by conducting a test loading without any liposomes. This test shows that upon complex formation of copper and EDTA, more than 96% of the copper in the sample is recovered in the filtrate. Solutions containing 720 μM copper (in HEPES buffer) or 720 μM copper and 1.0 mM DOTA (in HEPES buffer) was prepared. Together, these solutions and a sample of Cu-loaded liposomes were investigated using XAS.

X-ray Absorption Spectroscopy. The experimental and calculated XANES spectra of solvated Cu in HEPES buffer, Cu-DOTA, and Cu-loaded liposomes are shown in Figure 4A. The XANES spectra confirm the presence of copper in oxidation state +2 (Cu^{2+}) in all samples as seen by the absence of the characteristic pre-edge feature around 8983 eV occurring in the XANES spectra of copper in oxidation state +1.[24]

XANES spectra were calculated from different models in order to identify the $^{63}Cu^{2+}$-species present in the HEPES buffer sample. First, XANES spectra were calculated for different complexes in which Cu^{2+} is solely ligated by water in the following geometries: *i*) Jahn–Teller distorted six-coordinate $[Cu(H_2O)_6]^{2+}$, *ii*) regular five-coordinate square pyramidal $[Cu(H_2O)_5]^{2+}$, and *iii*) elongated five-coordinate square pyramidal $[Cu(H_2O)_5]^{2+}$ in which the four equatorial ligands were D_{2d}-distorted from the mean equatorial plane as shown in Figure 4B. This latter model shown in Figure 4B was adapted from the XAS solution structure of $[Cu(H_2O)_5]^{2+}$ at room temperature by Frank et al.[25] and results in a significantly better agreement with the measured XANES spectrum (R_{XANES} = 0.0217), as compared to the six-coordinate complex (R_{XANES} = 0.0384) and the regular five-coordinate square pyramidal complex (R_{XANES} = 0.0284). A 1.0% reduction of the Cu–O distances due to temperature differences further improved the fit as shown in Figure 4A (R_{XANES} = 0.0179).

After a few days, a precipitate was observed in the buffer sample. An X-ray powder diffraction analysis identified this precipitate as clinoatacamite, which is a monoclinic polymorph of dicopper trihydroxide chloride.[26] Clinoatacamite contains three crystallographically different copper atoms, of which three-quarters of them adopt a six-coordinate Jahn–Teller distorted geometry $[Cu(OH)_4Cl_2]^{4-}$, similar to that shown in Figure 4C, which is a strong indication of coordination of chloride to copper. A XANES spectrum was therefore calculated from this structure. This resulted in a very good agreement with the measured XANES spectrum, as some of the spectral features are better explained by this model compared to the Cu-aqua models. This includes improved fit of the subtle edge feature at 8990 eV as well as the shoulder around 9013 eV

DOI: 10.1021/acsami.5b04612
ACS Appl. Mater. Interfaces 2015, 7, 22796–22806

(Figure 4A). As the crystal structure was solved at room temperature shorter coordination distances were observed in the experimental XANES spectrum, and therefore an isotropic contraction of the unit cell of 2.0% was applied to optimize the fit (R_{XANES} = 0.0145). The orthorhombic crystal structure of the Cu-DOTA,[27] which is shown in Figure 4D was used to calculate the XANES spectrum of the Cu-DOTA complex. The fit was further improved by a 1.9% isotropic contraction of the unit cell in which R_{XANES} improved from 0.0214 to 0.0149.

A linear combination of the experimental spectra of solvated Cu^{2+} and Cu-DOTA was fitted to the experimental XANES spectrum of Cu-loaded liposome (R_{XANES} = 0.0064). The fit is shown in Figure 4A. The fraction of copper coordinated to DOTA was refined to 88%, which is in agreement with the loading of 93%. This concludes that Cu^{2+} is loaded into the liposomes, where it is chelated by DOTA.

3.4. Dependence on Lipid Composition and Activity. The new UAL method was tested for an extended set of liposome formulations listed in Table 1, and all were successfully loaded (%$load_{SEC}$ > 95%, %$load_{TLC}$ > 95%). The loading efficiency, evaluated by SEC and radio-TLC, is found to be independent of 1) DSPE-PEG_{2000} content for the stealth formulation, 2) targeting groups such as DSPE-PEG_{2000}-RGD and DSPE-PEG_{5000}-Folate, 3) the presence of cationic and anionic lipids, 4) cholesterol content and 5) lipid saturation or membrane phase-state (gel or fluid). Moreover, stealth liposomes were successfully loaded at low, medium, and high radioactivity levels (10–800 MBq/mL $^{64}Cu^{2+}$).

Table 1. Liposomal Formulations and Loading Conditions for Which Successful Unassisted Loading (UAL) of $^{64}Cu^{2+}$ Has Been Achieved (%$load_{SEC}$ > 95%, %$load_{TLC}$ > 95%)[a]

liposomal formulations (molar ratio)	loading conditions
Stealth liposomes	
HSPC:CHOL:DSPE-PEG_{2000} (56.5:38.2:5.3)	55 °C, 3.3–10 mM, 10–800 MBq/mL
DSPC:CHOL:DSPE-PEG_{2000} (50:40:10)	55 °C, 3.3–10 mM, 50–100 MBq/mL
Targeted stealth liposomes	
DSPC:CHOL:DSPE-PEG_{2000}:DSPE-PEG_{2000}-RGD (55:40:4:1)	55 °C, 3.3 mM, 50–200 MBq/mL
DSPC:CHOL:DSPE-PEG_{2000}:DSPE-PEG_{5000}-Folate (56.2:38.0:5.3:0.5)	55 °C, 3.3 mM, 50–200 MBq/mL
Cationic and anionic liposomes	
HSPC:CHOL:DSTAP:DSPE-PEG_{2000} (43.5:38:12.5:6)	55 °C, 3.3 mM, 50–200 MBq/mL
HSPC:CHOL:DSTAP:DSPE-PEG_{2000} (31:38:25:6)	55 °C, 3.3 mM, 50–200 MBq/mL
POPC:POPG:CHOL:DSPE-PEG_{2000} (35:40:20:5)	55 °C, 5 mM, 50–200 MBq/mL
DPPC:DPPG:DSPE-PEG_{2000} (55:40:5)	55 °C, 5 mM, 50–200 MBq/mL
Zwitterionic liposomes	
POPC (100)	40, 55 °C, 5 mM, 50–200 MBq/mL
POPC:CHOL (60:40)	55 °C, 5 mM, 50–200 MBq/mL
DPPC (100)	55 °C, 3.3 mM, 50–200 MBq/mL
DSPC:CHOL (60:40)	55 °C, 3.3 mM, 50–200 MBq/mL

[a]Loading conditions are specified as loading temperature, lipid concentration, and ^{64}Cu activity.

3.5. In Vivo and in Vitro Performance of ^{64}Cu-Liposomes. The *in vivo* performance of $^{64}Cu^{2+}$ loaded HSPC:CHOL:DSPE-PEG_{2000} (56.5:38.2:5.3) liposomes (prepared by the UAL method) was investigated in the xenograft FaDu tumor model. The mice were PET/CT scanned 10 min and 24 h postinjection, as shown in the PET/CT fusion images of Figure 5A–D.

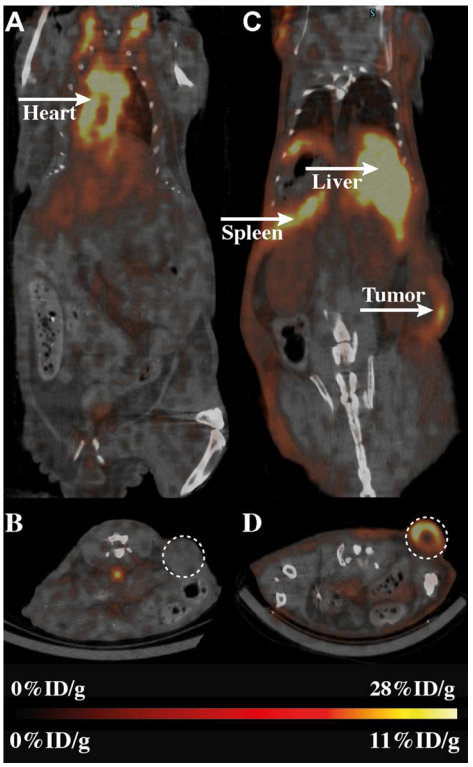

Figure 5. Coronal PET/CT image of FaDu tumor xenografts mice models injected with ^{64}Cu-liposomes (prepared using the UAL method). (A–B) Organ and tumor distribution 10 min postinjection of ^{64}Cu-liposomes and (C–D) 24 h postinjection. The activity in the heart represents ^{64}Cu-liposome activity in the blood of the heart chambers. The intensity scale bar presents the uptake in %ID/g and covers the range 0–28%ID/g in (A–B) and 0–11%ID/g in (C–D). The liposomes were composed of HSPC:CHOL:DSPE-PEG_{2000} in the molar ratio (56.5:38.2:5.3). The dashed circle in (B,D) defines the position of the tumor.

The blood, tumor, and organ accumulation, compiled in Table 2, has been quantified using PET imaging. Ten minutes postinjection, the ^{64}Cu-liposomes reside in the blood pool,

Table 2. Biodistribution Data for ^{64}Cu-Liposomes Administered to FaDu Tumor Bearing Mice (n = 5) and a Dog (n = 1)[a]

	mice		dog	
organs	%ID/g	SUV	%ID/kg	SUV
blood (10 min)	33 ± 4	10 ± 1		
blood (24 h)	6.4 ± 0.4	1.9 ± 0.1	12.0	5.7
liver (24 h)	13 ± 1	3.9 ± 0.3	7.9	3.8
spleen (24 h)	14 ± 2	4.2 ± 0.6	5.2	2.5
muscle (24 h)	0.4 ± 0.1	0.12 ± 0.03	0.4	0.2
tumor (24 h)	6 ± 2	1.8 ± 0.6	-	-

[a]The liposomes were composed of HSPC:CHOL:DSPE-PEG_{2000} in the molar ratio (56.5:38.2:5.3). Scans were performed 10 min or 24 h postinjection. Values are means ± SEM (n = 5).

DOI: 10.1021/acsami.5b04612
ACS Appl. Mater. Interfaces 2015, 7, 22796–22806

which is evident in Figure 5A where a high $^{64}Cu^{2+}$ radioactivity is observed in the region of the heart. Only little activity is observed in the tumor (Figure 5B) at this time point. After 24 h, the ^{64}Cu-liposomes accumulate in the spleen, liver, and tumor as indicated by high $^{64}Cu^{2+}$ radioactivity in tissues in Figure 5C and uptake data in Table 2. The ^{64}Cu-liposome content in the blood decreases from (33 ± 4) %ID/g at 10 min to (6.4 ± 0.4) %ID/g at 24 h, which corresponds to a half-life of $T_{1/2}$ = 9.7 h assuming monoexponential blood clearance. Assuming an average weight of 27.5 g and an average blood volume of 8% v/w, 73% of the injected dose is accounted for by the blood pool 10 min postinjection.

^{64}Cu-liposomes, prepared by the UAL method, were administered to a single large canine model, which in concordance with the diagnostic evaluation of disease status also provided information on the *in vivo* stability in a large animal model. PET/CT fusion images of the large canine model are shown in Figure 6 A–B, where the activity is located primarily in the region of the spleen, liver, and heart.

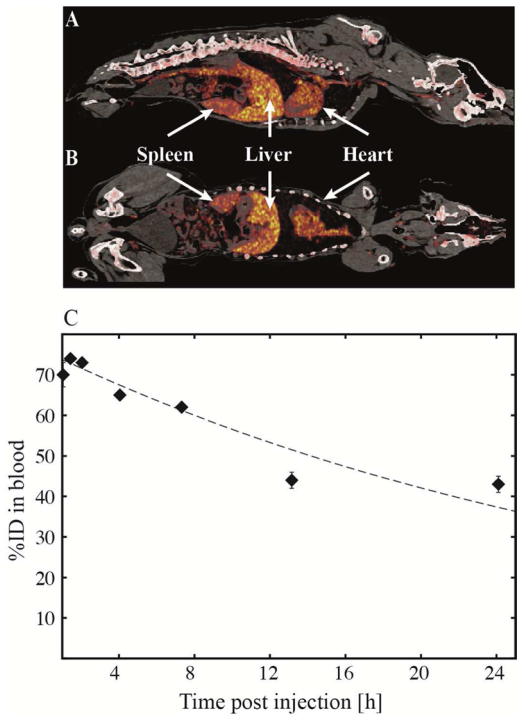

Figure 6. PET/CT image of a canine cancer model injected with ^{64}Cu-liposomes (prepared using the UAL method) 24 h postinjection. (A,B) Sagittal and coronal plane PET/CT images are shown with white arrows indicating the positions of the spleen, liver, and heart. The heart activity represents ^{64}Cu-liposome in the blood of the heart chambers. (C) The blood clearance profile is plotted as a function of time postinjection of ^{64}Cu-liposomes. The dashed line represents the fit of a monoexponential function. The error bars show the standard error of the mean (n = 3) and are not shown for error bars smaller than the symbols. The liposomes were composed of HSPC:CHOL:DSPE-PEG$_{2000}$ in the molar ratio (56.5:38.2:5.3).

SUVs and %ID/kg were quantified by PET imaging, and results are reported for tissues and blood in Table 2. The blood clearance profile, shown in Figure 6C, has been fitted using a monoexponential function, which yields a half-life of $T_{1/2}$ = 24 h ± 4 h. The monoexponential fit (Figure 6C) shows that the blood pool accounts for more than 75% of the injected dose at the time of injection.

Additionally, the *in vitro* stability of ^{64}Cu-liposomes, prepared by the UAL method, was investigated in human serum and canine and mice plasma (incubated for 18 h and at 37 °C) and was found to be very high with <5%, < 3%, and <2% leakage of ^{64}Cu-DOTA, in three separate experiments.

4. DISCUSSION

We have previously presented an efficient method for remote loading of $^{64}Cu^{2+}$ into liposomes using the ionophore 2HQ.[12] In this approach, copper is coordinated by 2HQ outside the liposomes, which lowers the kinetic energy barrier of crossing the lipid bilayer, and hence facilitates diffusion of the copper complex (Figure 1). Once inside the liposome, 2HQ is exchanged by entrapped chelators due to the copper affinity and excess chelator concentration. In the current study, a new method, excluding the use 2HQ or any other ionophore, is presented. In this UAL method, copper is added to liposomes entrapping a chelator, and, contrary to previous knowledge, copper spontaneously diffuses across the lipid bilayer where it is captured by the high affinity chelator (DOTA).

The new UAL method has major advantages compared to previously reported IAL methods,[4,7−12] because of its simplicity, excluding the use of any ionophore. The UAL method only requires an encapsulated chelator and proper incubation temperature to obtain high loading efficiencies (>95%) of radioactive $^{64}Cu^{2+}$ into liposomes. High loading efficiency (%load$_{SEC}$ > 95%, %load$_{TLC}$ > 95%) is obtained for a range of $^{64}Cu^{2+}$ activity levels, lipid concentrations, and composition (Table 1) thus highlighting the robustness and flexibility of the new loading method. In particular, loading efficiency is found not to depend on the presence of pegylated lipids, targeting ligands, liposome surface charge, or lipid phase state (gel or fluid). However, changes in surface potential/charge of liposomes are known to affect the spatial distribution of ions near the lipid membrane,[28,29] which could affect the loading efficiency of Cu^{2+}. Yet, no change in loading efficiency is observed for cationic HSPC:CHOL:DSTAP:DSPE-PEG$_{2000}$ (31:38:25:6) or anionic POPC:POPG:CHOL:DSPE-PEG$_{2000}$ (35:40:20:5) liposomes (Table 1) indicating that the membrane translocating copper species might be neutral. In work by Powel et al., speciation of copper in saline solution, in the presence of atmospheric CO_2 pressure, revealed $CuCO_3$(aq) to be the predominant form of copper at pH 7.4.[30] Oil/water-partitioning studies of copper, conducted by Blust and co-workers,[31] furthermore showed a dramatic increase in oil/water-partitioning of copper as pH was raised from 6.5 to 7.0. The latter result has been attributed to the formation of carbonate compounds by copper speciation. Both observations made by Powel and Blust fit our suggestion that copper is able to translocate the lipid bilayer in a charge independent manner. Our XANES analyses do not support the hypothesis of $CuCO_3$ being the dominant species in HEPES buffer. We see that copper is present either as a distorted five-coordinate square pyramidal $[Cu(H_2O)_5]^{2+}$ complex (Figure 4B) or adopt a coordination to chloride ($Cu(OH)_4Cl_2$) (Figure 4C) similar to that found in clinoatacamite. This difference might be explained by the larger concentration of copper and chloride used in the XAS experiment compared to the concentration used in the speciation calculation.[30] Liposome formulations with melting transition temperature below 55 °C have furthermore been successfully loaded at 55 °C. This indicates that little or no

DOI: 10.1021/acsami.5b04612
ACS Appl. Mater. Interfaces 2015, 7, 22796−22806

DOTA is leached from the liposome as a consequence of crossing the gel−fluid transition temperature.

The loading efficiency of the new UAL and the 2HQ IAL method is compared using SEC. The methods are compared at 30, 40, and 50 °C, which reveals a large difference in the temperature response of the loading efficiency (Figure 2). For the IAL method, the loading efficiency is found to be weakly dependent on temperature, whereas a larger response to changes in temperature is observed for the UAL method. This difference reflects a significant change in activation energy and hence a change in loading mechanism; an effect that might be attributed to altered transmembrane diffusion rate of the translocating copper species in the presence of 2HQ. An important observation is the lower loading efficiency obtained at 50 °C for the IAL method compared to the UAL method. Hence, the presence of 2HQ results in a free energy penalty of stripping copper from the ionophore, which shifts the loading reaction, Cu^{2+} (unloaded/free) ⇔ Cu^{2+} (loaded into liposome), toward the unloaded form. This argument is fully supported by the ligand exchange constant for the exchange of Cu^{2+} between 2HQ and DOTA determined in our recent work.[12]

In order to find the optimal loading conditions and elucidate the temperature response of the UAL method, loading kinetics has been investigated by radio-TLC. The loading rate (slope of $\%load_{TLC}$) and efficiency are found to be highly dependent on temperature, and an 8-fold increase in the initial loading rate is observed in response changing the temperature from 25 to 55 °C (Figure 3B). This change in initial rate correlates to the observed change in loading efficiency shown in Figure 2B and reflects the increased energy barrier for copper to cross the lipid bilayer unassisted. Despite the reduction in loading rate at room temperature, the loading still progresses and reached 36% after 1 h. At 55 °C incubation, 92% loading is obtained within 15 min, and >97% loading is achieved within 60 min; hence 55 °C was chosen as the optimal loading temperature. Furthermore, the obtained loading ($\%load_{TLC}$) evaluated at 60 min (Figure 3B) correlates with the loading efficiency obtained by SEC ($\%load_{SEC}$) shown in Figure 2B. Loading of $^{64}Cu^{2+}$ into empty liposomes resulted in highly reduced (or nearly negligible) loading efficiencies for both the IAL and UAL methods when compared to liposomes entrapping DOTA. The loading efficiency of empty liposomes furthermore scaled with the lipid concentration and agrees with the expected entrapped volume of 100 nm liposomes.

The UAL method has been investigated by XAS to identify copper species, which are likely to be involved in the loading process. Liposomes with a high DOTA content have been prepared and loaded with 720 μM Cu^{2+}, which show that even a large amount of copper can be loaded into liposomes using the UAL method. Analysis of XANES spectra (Figure 4A) confirms copper to be present in oxidation state +2 and to be coordinated to DOTA as expected upon loading into liposomes. In a HEPES buffer containing DOTA (1 mM) copper is concluded to be coordinated to DOTA (Figure 4D). A linear combination of the experimental spectra of solvated Cu^{2+} and Cu-DOTA has been fitted to the experimental XANES spectrum of copper loaded liposome (R_{XANES} = 0.0064, fit is shown in Figure 4A). From this fit, the fraction of copper coordinated to DOTA is refined to 88%, which is in agreement with the loading efficiency of 93% obtained by ICP-MS. This concludes that Cu^{2+} is loaded into the liposomes, where it is chelated by DOTA.

The *in vivo* performance of liposomes loaded with $^{64}Cu^{2+}$ using the UAL method has been assessed in small and large animal models. ^{64}Cu-liposomes were administered to mice bearing head and neck cancer xenografts, and accumulation in tissues of interest has been determined 10 min and 24 h postinjection (Figure 5). On PET images acquired 24 h postinjection, the liver, spleen, muscle, and tumor display liposome accumulation compatible to those recently published for stealth liposomes,[5,6,12] which demonstrates that the *in vivo* performance of liposomes loaded using the UAL method remains unchanged. The estimated blood circulation half-life of 9.7 h in mice is in agreement with earlier reports,[11,12,23] and no leakage of ^{64}Cu-DOTA from liposomes is observed in mice plasma (Figure S1). In addition, no activity was observed in the urinary bladder, and renal excretion was therefore considered negligible. Considering the size of the liposomes this is expectable for renal filtration, and it provides evidence that the liposomes were stable and did not leak ^{64}Cu-DOTA. Together, these results substantiate the *in vivo* stability of liposomes loaded with ^{64}Cu using the UAL method. These results furthermore support the hypothesis that stealth liposomes accumulate in tumors due to the EPR effect, which was also demonstrated in our recent work.[12]

Liposomes loaded with $^{64}Cu^{2+}$ using the UAL method were furthermore administered to a single canine model that has a body size and relative organ size and excretion kinetics comparable to humans. From PET/CT images, liposomes are found to accumulate in the spleen and liver 24 h postinjection as expected. Additionally, the large blood volume in the heart chambers displays high ^{64}Cu-liposome activity. The accumulation in organs and tissues 24 h postinjection has been determined via PET images, and SUVs of 3.8, 2.5, and 0.2 have been determined for the liver, spleen, and muscle, respectively. The blood clearance profile (Figure 6C) was determined upon administration of a single lipid dose (4.3 mg lipid/kg), which shows that more than 75% of the injected dose to be present in the blood pool at the time of injection. The obtained circulation half-life of 24 h, moreover, agrees with recent findings by Susuki and co-workers, who, upon administration of pegylated liposomes (6.7 μmol lipid/kg/5 mg lipid/kg), found an average half-life of 26 h in experimental beagle dogs.[32] Based on the long circulation half-life and lack of renal clearance, we conclude that the liposomes are stable and do not leak in canines. Such leakage would have resulted in rapid renal clearance of free Cu-DOTA, and if copper were to leave the Cu-DOTA complex a significantly decreased circulating half-life would have been observed.

With the increased recognition of the limitations in the use of SPECT for clinical liposome based imaging systems, improved radiolabeling methods are warranted, and especially methods useful in PET imaging are needed. In clinical application, ^{64}Cu-liposomes could potentially be useful in liposomal drug development, in cancer diagnostic imaging, and in various nanotheranostic applications such as in personalized medicine.[1,2] Thus, the unassisted $^{64}Cu^{2+}$ loading method and the *in vivo* performance of the ^{64}Cu-liposomal PET radiotracer presented here could eventually be useful in future clinical diagnostic and theranostic applications. An advantage of the UAL method is the ability to load clinically relevant activities of 200−400 MBq/patient[14] at robust and high loading efficiency (>97% for stealth liposomes), thereby reducing GMP production complexity as purification from free $^{64}Cu^{2+}$ or ^{64}Cu-DOTA can be avoided. In addition, removing the need for

DOI: 10.1021/acsami.5b04612
ACS Appl. Mater. Interfaces 2015, 7, 22796−22806

potentially toxic ionophores[33] for loading could potentially ease the regulatory approval needed for a clinical trial study. Changing from the IAL to the UAL method furthermore allows for formulating the liposomes at neutral internal pH, which reduces the risk of lipid hydrolysis during long-term storage. The UAL method is versatile and works independently of the lipid composition due to the employed gradient method, contrary to the other gradient methods that are affected e.g. by liposome surface charges. In recent work, Lee and co-workers published a method for remote loading of $^{64}Cu^{2+}$ using the pH sensitive chelator.[1] Their approach allows for remote coloading of a drug and PET tracer into the same liposome by use of a single pH gradient. However, the intrinsic thermodynamic loading stability/potential of the pH gradient method is significantly lower than that of the DOTA gradient used in the UAL method, resulting in lower encapsulation efficiencies of 90%[1] and potentially in only semiquantitative biodistribution analysis. Methods for surface chelation of $^{64}Cu^{2+}$ onto liposomes have been developed by Seo and co-workers, yielding similar results as for the UAL method.[5,6] However, the advantages of the UAL method are numerous as (1) it has a lower risk of transmetalation since Cu-DOTA resides inside the aqueous lumen of the liposome, (2) it does not suffer from lipid-chelator migration/exchange, and (3) it does not require surface modification that may affect targeting or clearance of these liposomes by the immune system.

5. CONCLUSION

We have successfully developed a highly efficient method for loading the PET radionuclide $^{64}Cu^{2+}$ into liposomes. The new UAL method relies on unassisted transport of copper ions across the lipid bilayer of liposomes entrapping a chelator. We demonstrate highly efficient loading (>95%) for a range of lipid formulations, which suggests that copper forms a neutral species capable of crossing the liposomal bilayer.

^{64}Cu-liposomes prepared by UAL show high tumor accumulation in mice and long-term blood circulation in a canine cancer model in agreement with previous biodistribution reports on the liposomal formulation. We observe that liposomes prepared by UAL or IAL have equivalent biodistribution and stability *in vitro* and *in vivo*.

This new Cu^{2+} unassisted loading method is simple, cost-efficient, robust, and highly thermodynamically stable with respect to radionuclide retention, contrary to surface chelation strategies that require tailored synthesis of lipid-chelator analogues and may suffer activity loss due to transmetalation or migration of lipidated chelators *in vivo*. The loading stability of the UAL method is superior to other remote loading strategies that rely on pH or other chemical gradients, due to the high binding affinity of DOTA, which is a strong asset of the new method.

Contrary to what has been common knowledge and practice in the field of radionuclide liposome loading, we have developed an extremely simple and powerful tool for loading $^{64}Cu^{2+}$ into liposomes without the use of ionophores. The method provides ^{64}Cu-liposomes with superior imaging properties due to the protected location of $^{64}Cu^{2+}$ inside the liposomes, which prohibits $^{64}Cu^{2+}$ exchange with the biological environment due to the protective barrier constituted by the liposome membrane. Thus, the ^{64}Cu-liposomes constitute a highly sensitive PET tracer useful in characterizing the *in vivo* performance of liposome based nanomedicine with great potential in clinical cancer diagnostic imaging applications as well as in various theranostic applications.

■ ASSOCIATED CONTENT

Supporting Information

The Supporting Information is available free of charge on the ACS Publications website at DOI: 10.1021/acsami.5b04612.

Figure S1 (PDF)

■ AUTHOR INFORMATION

Corresponding Author

*Phone: 45 45258168. E-mail: thomas.andresen@nanotech.dtu.dk.

Notes

The authors declare no competing financial interest.

■ ACKNOWLEDGMENTS

The Danish Strategic Research Council, the Technical University of Denmark (DTU), the Danish National Advanced Technology Foundation, European Research Council (ERC), and the Lundbeck Foundation kindly provided financial support of this project.

■ REFERENCES

(1) Lee, H.; Cheng, J.; Gaddy, D.; Orcutt, K. D.; Leonard, S.; Geretti, E.; Hesterman, J.; Harwell, C.; Hoppin, J.; Jaffray, D. A.; Wickham, T.; Hendriks, B. S.; Kirpotin, D. A Gradient-loadable ^{64}Cu-chelator for Quantifying Tumor Deposition Kinetics of Nanoliposomal Therapeutics by Positron Emission Tomography. *Nanomedicine* **2015**, *11*, 155−165.

(2) Petersen, A. L.; Hansen, A. E.; Gabizon, A.; Andresen, T. L. Liposome Imaging Agents in Personalized Medicine. *Adv. Drug Delivery Rev.* **2012**, *64*, 1417−1435.

(3) Goins, B. A. Radiolabeled Lipid Nanoparticles for Diagnostic Imaging. *Expert Opin. Med. Diagn.* **2008**, *2*, 853−873.

(4) Gabizon, A.; Huberty, J.; Straubinger, R. M.; Price, D. C.; Papahadjopoulus, D. An Improved Method for In Vivo Tracing and Imaging of Liposomes using a Gallium 67− Deferoxamine Complex. *J. Liposome Res.* **1988**, *1*, 123−135.

(5) Seo, J. W.; Mahakian, L. M.; Kheirolomoom, A.; Zhang, H.; Meares, C. F.; Ferdani, R.; Anderson, C. J.; Ferrara, K. W. Liposomal Cu-64 Labeling Method using Bifunctional Chelators: Polyethylene Glycol Spacer and Chelator Effects. *Bioconjugate Chem.* **2010**, *21*, 1206−1215.

(6) Seo, J. W.; Qin, S.; Mahakian, L. M.; Watson, K. D.; Kheirolomoom, A.; Ferrara, K. W. Positron Emission Tomography Imaging of the Stability of Cu-64 Labeled Dipalmitoyl and Distearoyl Lipids in Liposomes. *J. Controlled Release* **2011**, *151*, 28−34.

(7) Bao, A.; Goins, B.; Klipper, R.; Negrete, G.; Phillips, W. Direct ^{99m}Tc Labeling of Pegylated Liposomal Doxorubicin (Doxil) for Pharmacokinetic and Non-Invasive Imaging Studies. *J. Pharmacol. Exp. Ther.* **2004**, *308*, 419−425.

(8) Boerman, O.; Storm, G.; Oyen, W.; Vanbloois, L.; Vandermeer, J.; Claessens, R.; Crommelin, D. J.; Corstens, F. H. Sterically Stabilized Liposomes Labeled with In-111 to Image Focal Infection. *J. Nucl. Med.* **1995**, *36*, 1639−1644.

(9) Hwang, K.; Merriam, J.; Beaumier, P.; Luk, K. Encapsulation, with High-efficiency, of Radioactive Metal-ions in Liposomes. *Biochim. Biophys. Acta, Gen. Subj.* **1982**, *716*, 101−109.

(10) Mougin-Degraef, M.; Jestin, E.; Bruel, D.; Remaud-Le Saec, P.; Morandeau, L.; Faivre-Chauvet, A.; Barbet, J. High-activity Radioiodine Labeling of Conventional and Stealth Liposomes. *J. Liposome Res.* **2006**, *16*, 91−102.

(11) Wang, H.-E.; Yua, H.-M.; Lua, Y.-C.; Heishe, N.-N.; Tseng, Y.-L.; Huang, K.-L.; Chuang, K.-T.; Chen, C.-H.; Hwang, J.-J.; Lin, W.-J.;

DOI: 10.1021/acsami.5b04612
ACS Appl. Mater. Interfaces 2015, 7, 22796−22806

Wang, S.-J.; Ting, G.; Whang-Peng, J.; Deng, W.-P. Internal Radiotherapy and Dosimetric Study for $^{111}In/^{177}Lu$-pegylated Liposomes Conjugates in Tumor-bearing Mice. *Nucl. Instrum. Methods Phys. Res., Sect. A* **2006**, *569*, 533−537.
(12) Petersen, A. L.; Binderup, T.; Rasmussen, P.; Henriksen, J. R.; Elema, D. R.; Kjær, A.; Andresen, T. L. ^{64}Cu Loaded Liposomes as Positron Emission Tomography Imaging Agents. *Biomaterials* **2011**, *32*, 2334−2341.
(13) Locke, L. W.; Mayo, M. W.; Yoo, A. D.; Williams, M. B.; Berr, S. S. PET Imaging of Tumor Associated Macrophages using Mannose Coated ^{64}Cu Liposomes. *Biomaterials* **2012**, *33*, 7785−7793.
(14) Gaddy, D. F.; Lee, H.; Zheng, J.; Jaffray, D. A.; Wickham, T. J.; Hendriks, B. S. Whole-body organ-level and kidney micro-dosimetric evaluations of 64Cu-loaded HER2/ErbB2- targeted liposomal doxorubicin (64Cu-MM-302) in rodents and primates. *EJNMMI Res.* **2015**, *5*, 24.
(15) Hauser, H.; Phillips, M. C.; Stubbs, M. Ion Permeability of Phospholipid Bilayers. *Nature* **1972**, *239*, 342−344.
(16) Mills, J. K.; Needham, D. Lysolipid Incorporation in Dipalmitoylphosphatidylcholine Bilayer Membranes Enhances the Ion Permeability and Drug Release Rates at the Membrane Phase Transition. *Biochim. Biophys. Acta, Biomembr.* **2005**, *1716*, 77−96.
(17) Papahadjopoulos, D.; Nir, S.; Ohki, S. Permeability Properties of Phospholipid Membranes: Effect of Cholesterol and Temperatures. *Biochim. Biophys. Acta, Biomembr.* **1971**, *266*, 561−583.
(18) Paula, S.; Volkov, A. G.; Deamer, D. W. Permeation of Halide Anions through Phospholipid Bilayers occurs by the Solubility-diffusion Mechanism. *Biophys. J.* **1998**, *74*, 319−327.
(19) Carlson, S.; Clausén, M.; Gridneva, L.; Sommarin, B.; Svensson, C. XAFS Experiments at Beamline I811, MAX-lab synchrotron source, Sweden. *J. Synchrotron Radiat.* **2006**, *13*, 359−364.
(20) Frankær, C. G.; Harris, P.; Ståhl, K. A Sample Holder for In-house X-ray Powder Diffraction Studies of Protein Powders. *J. Appl. Crystallogr.* **2011**, *44*, 1288−1290.
(21) Ressler, T. WinXAS: A Program for X-ray Absorption Spectroscopy Data Analysis under MS-Windows. *J. Synchrotron Radiat.* **1998**, *5*, 118−122.
(22) Joly, Y. X-ray Absorption Near-edge Structure Calculations beyond the Muffin-tin Approximation. *Phys. Rev. B: Condens. Matter Mater. Phys.* **2001**, *63*, 1251201−1251210.
(23) Petersen, A. L.; Binderup, T.; Jølck, R. I.; Rasmussen, P.; Henriksen, J. R.; Pfeifer, A. K.; Kjær, A.; Andresen, T. L. Positron Emission Tomography Evaluation of Somatostatin Receptor Targeted ^{64}Cu-TATE-Liposomes in a Human Neuroendocrine Carcinoma Mouse Model. *J. Controlled Release* **2012**, *160*, 254−263.
(24) Kau, L. S.; Spira-Solomon, D. J.; Penner-Hahn, J. E.; Hodgson, K. O.; Solomon, E. I. X-ray Absorption Edge Determination of the Oxidation State and Coordination Number Application to the Type 3 site in Rhus-vernicifera Laccase and its Reaction with Oxygen. *J. Am. Chem. Soc.* **1987**, *109*, 6433−6442.
(25) Frank, P.; Benfatto, M.; Szilagyi, R. K.; D'Angelo, P.; Della Longa, S.; Hodgson, K. O. The Solution Structure of [Cu(aq)](2+) and its Implications for Rack-Induced Bonding in Blue Copper Protein Active Sites. *Inorg. Chem.* **2007**, *46*, 7684−7684.
(26) Grice, J. D.; Szymanski, J. T.; Jambor, J. L. The Crystal Structure of Clinoatacamite, a New Polymorph of Cu-2(OH)(3)Cl. *Can. Mineral.* **1996**, *34*, 73−78.
(27) Riesen, A.; Zehnder, M.; Kaden, T. A. Metal-Complexes of Macrocyclic Ligands 24. Binuclear Complexes with Tetraazamacrocycle-N,N′,N″,N‴-tetraacetic Acids. *Helv. Chim. Acta* **1986**, *69*, 2074−2080.
(28) McLaughlin, S. The Electrostatic Properties of Membranes. *Annu. Rev. Biophys. Biophys. Chem.* **1989**, *18*, 113−136.
(29) Etzerodt, T.; Henriksen, J. R.; Rasmussen, P.; Clausen, M. H.; Andresen, T. L. Selective Acylation Enhances Membrane Charge Sensitivity of the Antimicrobial Peptide Mastoparan-X. *Biophys. J.* **2011**, *100*, 399−409.
(30) Powell, K. J.; Brown, P. L.; Byrne, R. H.; Gajda, T.; Hefter, G.; Sjöberg, S.; Wanner, H. Chemical Speciation of Environmentally Significant Metals with Inorganic Ligands. *Pure Appl. Chem.* **2007**, *79*, 895−950.
(31) Blust, R.; Bernaerts, F.; Linden, A. V.; Thoeye, C. In *Artemia Research and its Application*; Sorgeloos, P., Bengtson, D. A., Decleir, W., Jaspers, E., Eds.; Universa Press: Wetteren, Belgium, 1987; pp 311−323.
(32) Suzuki, T.; Ichiharab, M.; Hyodoa, K.; Yamamotoa, E.; Ishidab, T.; Kiwada, H.; Ishihara, H.; Kikuchi, H. Accelerated Blood Clearance of PEGylated Liposomes Containing Doxorubicin upon Repeated Administration to Dogs. *Int. J. Pharm.* **2012**, *436*, 636−643.
(33) Kart, A.; Bilgili, A. Ionophore Antibiotics: Toxicity, Mode of Action and Neurotoxic Aspect of Carboxylic Ionophores. *J. Anim. Vet. Adv.* **2008**, *7*, 748−751.

DOI: 10.1021/acsami.5b04612
ACS Appl. Mater. Interfaces 2015, 7, 22796−22806